Modelling, Design, Control, and Implementation of a Modified Z-source Integrated PV/Grid/EV DC Charger/Inverter

Siddhartha A. Singh, *Student Member*, *IEEE*, Giampaolo Carli, *Member*, *IEEE*, Najath A. Azeez, *Member*, *IEEE*, and Sheldon S. Williamson, *Senior Member*, *IEEE*

***Abstract*—Solar Energy has been the most popular sources of renewable energy for residential and semi commercial applications. Fluctuations of solar energy harvested due to atmospheric conditions can be mitigated through energy storage systems. Solar energy can also be used to charge electric vehicle batteries to reduce the dependency on the grid. One of the requirements for a converter for such applications is to have a reduced number of conversion stages and provide isolation. Z-source inverter (ZSI) topology is able to remove multiple stages and achieve voltage boost and DC-AC power conversion in a single stage. The use of passive components also presents an opportunity to integrate energy storage systems (ESS) into them. This paper presents modeling, design and operation of a modified Z-source inverter (MZSI) integrated with a split primary isolated battery charger for DC charging of electric vehicles (EV) batteries. Simulation and experimental results have been presented for the proof of concept of the operation of the proposed converter.**

***Index Terms*—Z-source-inverters;Active filter; energy storage; photovoltaic (PV) power generation; quasi-Z-source inverter (qZSI); single-phase systems; transportation electrification; Solar energy; distributed power generation,inverter.**

I. Introduction

CHARGING of electric vehicles at present heavily involve the use AC grid. The various methods of charging exclusively use AC grid, such as wireless charging or plug-in charging can still cause pollution irrespective of how highly efficient the topology is. The amount of fossil fuels that are consumed to generate the energy to charge an electric vehicle gives a clearer picture of the carbon footprint that is left behind while charging an electric vehicle. To achieve lower carbon footprints, one of the ways is to integrated renewable energy sources into a charging infrastructure to reduce the dependency on the AC grid.

Manuscript received July 31, 2017; revised September 12, 2017; accepted November 22, 2017.

Siddhartha A. Singh, Najath A. Azeez and Sheldon S. Williamson are with Smart Transportation Electrification and Energy Research Group, Department of Electrical, Computer, and Software Engineering, University of Ontario Institute of Technology, Oshawa, ON, Canada (e-mail: siddhartha.anirban87@gmail.com; najath@gmail.com; sheldon.williamson@uoit.ca).

Giampaolo Carli is with EMD Technologies in Saint-Eustache, Canada. (e-mail:giampaolocarli@gmail.com)

A major requirement for designing an EV battery charger is the use of isolation transformers in the converter topologies, to provide galvanic isolation at the user end from the rest of the high voltage (HV) system as a safety measure [1].

The galvanic isolation can be provided either on the AC grid side or on the charger side. The size of the isolation transformer on the grid side is usually much larger than the one on the charger side [2]. Due to the improvement in semiconductor technology, high frequency switching facilitates the use of smaller size transformers for galvanic isolation.

Photovoltaic grid interconnected systems have been used in the past for commercial charging infrastructure [3]. These systems reduce the dependency of the charging infrastructure on the AC grid. The use of solar and grid interconnected system is an attractive solution for residential charging systems for EVs. For systems upto 10 kW, single phase inverters can be used for residential applications [4][5]. For interconnection of the residential solar PV to the grid, various isolated and non isolated topologies are available with multiple stages [4]-[6]. Residential photovoltaic systems for EV charging require features such as isolation and voltage boost capabilty to match the solar PV array voltage to the grid voltage requirements.

The ZSI topology was first introduced in [7]. It has an ability to buck or boost and invert the input DC voltage in a single stage. It has gained tremendous interest in photovoltaic-grid connected applications. The ZSI topology uses two capacitors and two inductors to boost the input DC voltage to match the inverter side AC output voltage requirements. The operation of a ZSI is heavily dependent on the passive components. It presents an opportunity to integrate energy storage units into such a system.

In this paper a proof of concept of a single phase MZSI based solar grid connected charger has been presented as an application towards a string inverter configuration. In section II, the basic operation principle for a ZSI have been discussed along with the component design. Section III, discusses the sizing of components, modeling and control of the converter. Section IV, presents the simulation results for the operation of a 3.3 kW proposed inverter charger and results from an experimental setup built as a proof of concept. Section V, presents the conclusion.

This article has been accepted for publication in a future issue of this journal, but has not been fully edited. Content may change prior to final publication. Citation information: DOI 10.1109/TIE.2017.2784396, IEEE Transactions on Industrial Electronics

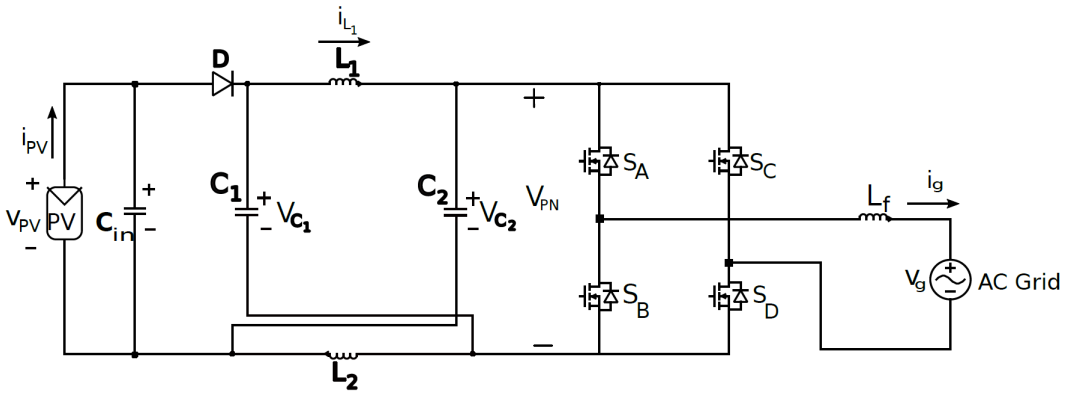

Fig. 1. Schematic of a Photovoltaic/AC grid inter- connected Z-source Inverter(ZSI)

II. TRADITIONAL ZSI

The ZSI topology, shown in Fig.1, utilizes two modes of operation: the shoot through state and the non shoot through state [7]. For symmetrical operations,

$$i_L = i_{L1} = i_{L2} \tag{1}$$

$$V_C = V_{C1} = V_{C2} \tag{2}$$

From Fig.1, in the shoot through state, all four switches, S_1, S_3, S_2 and S_4, are conducting at the same time. The duration of this shoot through state is described by the duty cycle D_0 and the switching frequency F_{SW}.

The shoot through state can be implemented by a modified PWM technique presented in [7].

Therefore, the two capacitor voltages are expressed as [7]:

$$V_C = \frac{1 - D_0}{1 - 2D_0} v_{pv} \tag{3}$$

Thus, maintaining a higher peak voltage at the input of the DC link, V_{PN}. The peak DC link voltage, $\hat{V_{PN}}$, is given by [7]:

$$\hat{V_{PN}} = \frac{1}{1 - 2D_0} v_{pv} \tag{4}$$

The power balance equation between the DC and AC side of the ZSI is expressed as [7],

$$(1 - D_0)\hat{V_{PN}} I_{PN} = i_{grms} v_{grms} \tag{5}$$

where I_{PN} and $\hat{V_{PN}}$ are the peak DC link current and voltage. The peak AC voltage of the ZSI is [7]:

$$V_g = M\hat{V_{PN}} \tag{6}$$

where the M is the modulation index, grid voltage, v_g=$V_g$sinωt and the grid current i_g=$I_g$sin(ωt+ϕ). For ϕ=0 for grid connected applications. From equation (11) and (13) the RMS of the output AC voltage of the ZSI is [7]:

$$V_{grms} = \frac{M v_{pv}}{\sqrt{2}(1 - 2D_0)} \tag{7}$$

III. COMPONENT SIZING, MODELING AND CONTROL OF PROPOSED MZSI

Fig. 2 shows a modified Z source inverter has been proposed having an integrated charger. The two capacitors C_1 and C_2 from Fig.1 are split and each of them act as one of the legs of one of the two primaries of the split primary isolated half bridge converter. The MOSFET S_R allows bidirectional operation of the MZSI when required. The diode D_{PV} blocks the reverse flow of current back into the PV. R_{in} is the internal resistance of the input capacitor C_{in}. For symmetrical operation of the MZSI, a split primary isolated DC to DC converter has been proposed for the integration of the charger side into the ZSI. The split primaries contain two half bridge converter (HBC) primaries isolated from a single full bridge secondary through a high frequency transformer. The HBC primaries and the secondaries are operated at 50% duty cycle in open loop. The output current of the secondary is connected to a energy storage unit such as a lithium-ion (Li-ion) battery. The energy storage unit clamps its own voltage, v_B, across the input of the HBC primaries, V_C, such that,

$$V_C = 2v_B \tag{8}$$

A. Maximum Shoot Through Duty Ratio, D_{0max}

As a result of the energy storage unit being connected across the capacitors, the maximum shoot through duty ratio, D_{0max} is calculated based on the minimum input voltage, v_{pvmin} and the maximum battery voltage, V_{Bmax} connected across the capacitors and is expressed as:

$$D_{0max} = \frac{2V_{Bmax} - v_{pvmin}}{4V_{Bmax} - v_{pvmin}} \tag{9}$$

SAE J1772 standard defines the standard battery voltages for DC charging between 200V-500V.

B. Inductor L_1 and L_2 design

The inductors L_1 and L_2 are sized for high frequency peak to peak current ripple assumed between 15-25% of the

This article has been accepted for publication in a future issue of this journal, but has not been fully edited. Content may change prior to final publication. Citation information: DOI 10.1109/TIE.2017.2784396, IEEE Transactions on Industrial Electronics

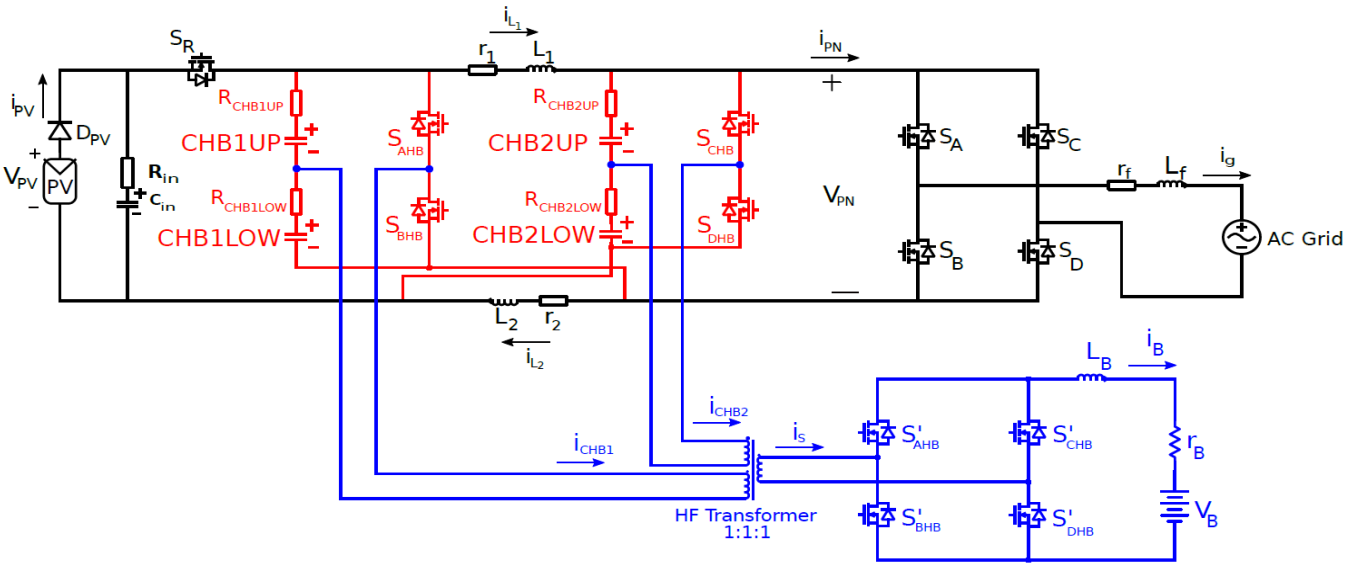

Fig. 2. Detailed Schematic of Proposed MZSI

inductor current during the shoot-through time interval $\frac{D_0 T}{2}$ as follow [8]:

$$L_1 = L_2 = \frac{V_{Cmax} D_{0max}}{2\Delta i_L f} \tag{10}$$

C. Capacitor C_1 and C_2 design

The capacitors are sized to absorb the second order harmonic component in the capacitor voltages as follow [8]:

$$C_1 = C_2 = \frac{P}{2\omega \Delta V_C V_C} \tag{11}$$

where V_C is the average voltage across the capacitors V_{C1} and V_{C2} and ΔV_C is the predetermined voltage ripple limit. ω is the second order harmonics expressed in rad/s.

In single phase Z source inverters, oversized electrolytic capacitors for second order harmonics suppression can result in a bulky system. A DC side Active Power Filter(APF) proposed in [9], can be used to reduce the capacitance required. It operates independent of the operation of the MZSI.

For the proposed topology, maximum capacitor voltage rating is equal to atleast twice the peak voltage of the energy storage device clamped across it.

D. Average Modeling of the Integrated Half-Bridge DC-DC Converter Charger

When a energy storage unit is connected to the secondary side of the charger then each of the split primaries operates alternately and supplies half the required battery current. Each of the primaries of the DC-DC converter is connected across the capacitors of either legs. The voltage across the capacitors is defined by the equation (15). The detailed average modeling of the split primary DC-DC converter is explained in [10]. Each of the two primaries can be represented using a RLE circuit connected parallel to each of the capacitor, C_1 and C_2, as shown in the simplfied equivalent model of the the Fig.4.

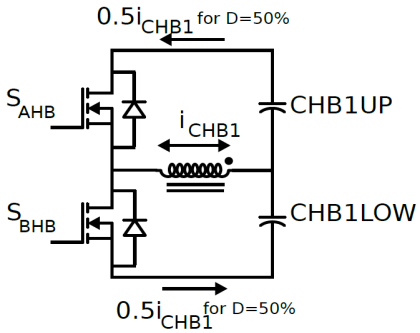

Fig. 3. Schemetic of one the Primary across CHB1 operating at 50% duty cycle.

E. State Space Average Modeling of the Single Stage Inverter Charger

The detailed state space average modeling was presented in [10]. The equivalent diagram of the modeled MZSI is ahown in the Fig. 4, During the non shoot-through state, the KVL equation is given by:

$$L\frac{di_L}{dt} = v_{pv} - i_L r + R_{HB} + (2\hat{i_g} + \frac{i_B}{2})R_{HB} - V_C \tag{12}$$

The KCL equation is:

$$C\frac{dV_C}{dt} = i_L - \hat{i_g} - \frac{i_B}{4} \tag{13}$$

During the shoot-through state, the KVL equation is:

$$L\frac{di_L}{dt} = V_C - i_L(R_{HB} + r) - \frac{i_B}{2}R_{HB} \tag{14}$$

The KCL equation is written as:

$$C\frac{dV_C}{dt} = -i_L - \frac{i_B}{4} \tag{15}$$

This article has been accepted for publication in a future issue of this journal, but has not been fully edited. Content may change prior to final publication. Citation information: DOI 10.1109/TIE.2017.2784396, IEEE Transactions on Industrial Electronics

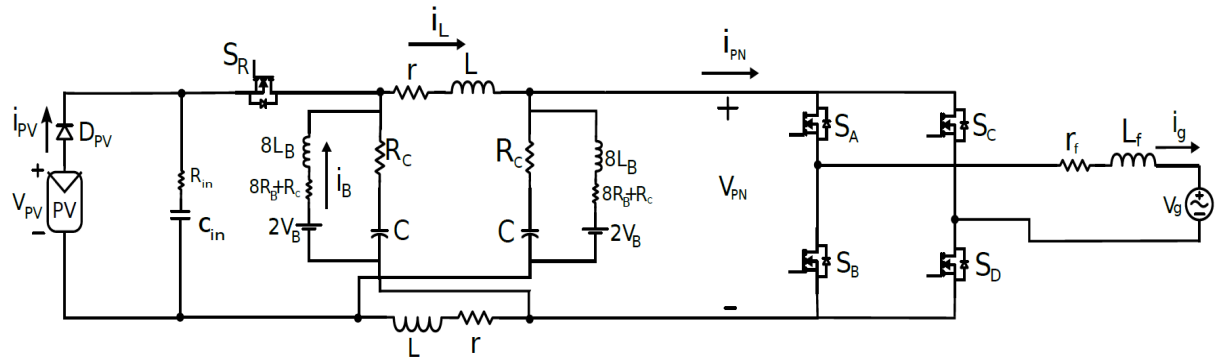

Fig. 4. Equivalent Model of the proposed Modified Z-source Inverter(MZSI) with battery

From equation (12)-(15), state space equations for the entire system can be written as:

$$\begin{bmatrix} \dot{i_L} \\ \dot{V_C} \\ \dot{i_B} \end{bmatrix} = \begin{bmatrix} -\frac{-(r+2R_{HB})}{L} & -\frac{1-2D_0}{L} & \frac{(1-2D_0)}{2}R_{HB} \\ \frac{1-2D_0}{C} & 0 & -\frac{1}{4C} \\ \frac{1-2D_0}{L_B}R_{HB} & \frac{1}{2L_B} & -\frac{R_{HB}+R_B}{2L_B} \end{bmatrix} \begin{bmatrix} i_L \\ V_C \\ i_B \end{bmatrix} + \begin{bmatrix} \frac{2(1-D_0)R_{HB}}{L} \\ -\frac{1-D_0}{C} \\ -\frac{(1-D_0)R_{HB}}{L_B} \end{bmatrix} \begin{bmatrix} i_d \end{bmatrix} + \begin{bmatrix} \frac{(1-D_0)}{L} \\ 0 \\ 0 \end{bmatrix} \begin{bmatrix} v_{pv} \end{bmatrix} + \begin{bmatrix} 0 \\ 0 \\ -\frac{1}{L_B} \end{bmatrix} \begin{bmatrix} V_B \end{bmatrix} \quad (16)$$

Fig. 4 shows the positive directions of the battery current, i_B, and the grid side AC current, i_g.

Fig. 5 shows the block diagram for the controller for the proposed MZSI topology. It consists of three loops: the PV current i_{pv} loop, grid current i_g loop and the battery current i_B loop.

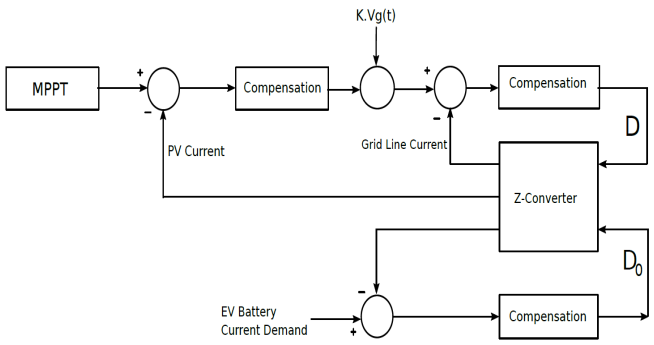

Fig. 5. Block diagram of the Control Scheme Proposed Modified Z-source Inverter Charger

In literature, the ZSI capacitor voltage is controlled to generate the reference current for the H-bridge inverter output current [11] or generate the shoot through duty ratio D_0 [12]. In this paper the reference current is generated by controlling the peak input photovoltaic current [13]. If a stiff voltage V_C is connected across either or both capacitors, the shoot through duty ratio, D_0, will depend on V_C.

Since the battery current loop do not require fast dynamic changes battery loop control is the slowest response compared to the input current control. For the battery loop control the transfer function is given by:

$$\frac{I_B(s)}{d_0(s)} = \frac{-sC[4R_{HB}i_L - 2R_{HB}i_d] - [2i_L - i_d]}{2L_BCs^2 + sC[R_{HB} + 2R_B] + 0.25} \quad (17)$$

A feedforward is added to the battery control loop,

$$FF_B = \frac{2V_B - v_{PV}}{4V_B - v_{PV}} \quad (18)$$

where V_B is the output voltage of the HBC and v_{PV} is the tracked PV voltage.

The output AC side current controller should have the fastest response.

F. Energy Management Scheme for the Proposed Converter

Fig. 6 shows a simplified block diagram of the proposed system. When an ESS is integrated into a ZSI, the equation (5) is modified as follows [14]:

$$v_{PV}i_{PV} = v_bi_b + i_{grms}v_{grms} \quad (19)$$

where i_b and v_b are the battery and voltage. Fig. 6 shows that the single phase AC grid power P_g balances the power fluctuation of the photovoltaic source P_{pv} thus a constant charge power, P_B, is obtained at the ESS.

For EV battery charging using both the single phase AC grid and the photovoltaic power, the direction of the AC grid current i_g changes to negative while drawing power from the grid.

The inverter side can be operated bidirectionally and the PV and the grid provides power for the charger, maintaining the power balance.

$$v_{PV}i_{PV} + i_{grms}v_{grms} = v_bi_b \quad (20)$$

This article has been accepted for publication in a future issue of this journal, but has not been fully edited. Content may change prior to final publication. Citation information: DOI 10.1109/TIE.2017.2784396, IEEE Transactions on Industrial Electronics

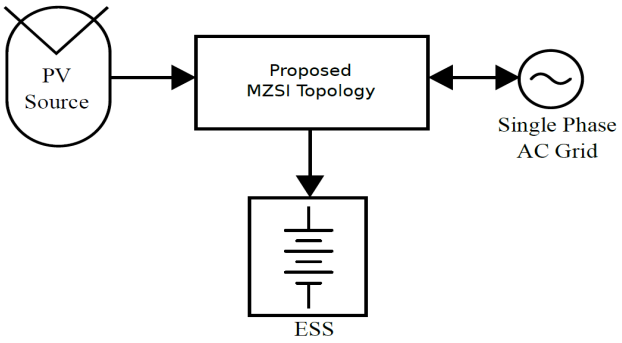

Fig. 6. Simplified Block Diagram of the System

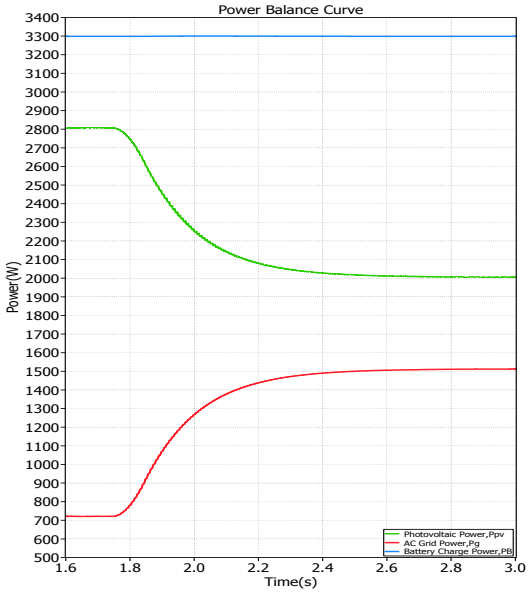

Fig. 7. Simulation Waveform for the power balance between the Photovoltaic input power, the AC Grid side and the battery power.

As long as the voltage across the input capacitor C_{in} is maintained to atleast the minimum value of the PV voltage, the MZSI can be operated as a grid connected rectifier/charger in the absence of the PV [15]-[16].

Anti-islanding protection techniques for the ZSI topology have been addressed in literature previously in [17].

IV. Simulation and Experimental Results

A. Simulation study for a MZSI operation

The simulation studies to demonstrate the behaviour of the proposed topology have been carried out using PLECS 4 for a 3.3 kW charger for a string inverter configuration. Simulation has been carried out for the system shown in Fig.2.

Fig.7 shows at simulation time t=1.75 s, the input PV power reduces from 2.8 kW to 2 kW, the grid power increases from 710 W to 1500 W to maintain the output charger power to 3.3kW and the corresponding grid current, DC link voltage, capacitor voltage and the battery current is shown in Fig.8.

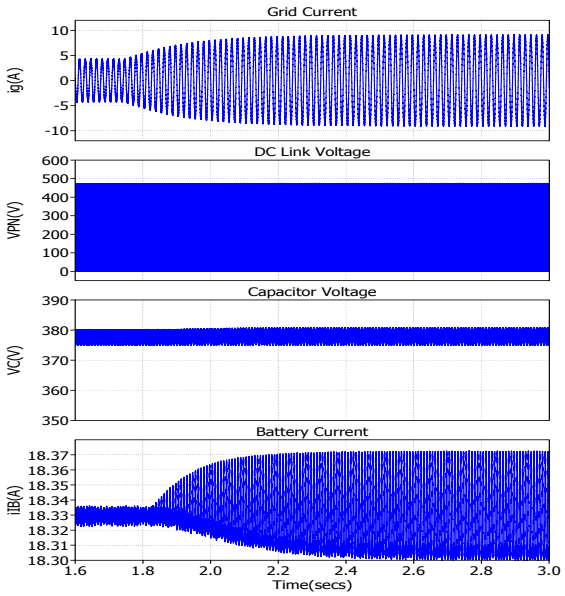

Fig. 8. Simulation Waveform of the grid current,I_g, DC link voltage,V_{PN}, Capacitor Voltage,V_{C1}, and Battery current,i_b for the power balance between the Photovoltaic input power, the AC Grid side and the battery power.

TABLE I
Modified ZSI based Charger System Simulation Specifications

Parameters	Value
Input Voltage, V_{in}	286 V
Input Current, I_{in}	9.8 A
Inductor Value, L_1=L_2	500 uH
ZSI Switching Frequency, F_{SW}	25 kHz
Grid Voltage (RMS), V_g	240 V
Inverter Output Filter Inductor, L_f	7.5 mH
PV Input Power, P_{PV}	2.8 kW
Input Capacitor, C_{in}	2 mF
HBC Switching Frequency, f	50 kHz
HBC Output Filter, L_B	1 mH
Battery charge power, P_B	3.3 kW

TABLE II
Component Models used for Loss Modeling of the Proposed System

Component	Value
Diode, D	STTH6010W
ZSI MOSFETs [S_A, S_B, S_C and S_D]	APT28M120L
HBC MOSFETs [S_{AHB}, S_{BHB}, S_{CHB} and S_{DHB}]	APT28M120L
HBC Diodes, [S'_{AHB}, S'_{BHB}, S'_{CHB} and S'_{DHB}]	STTH6010W
Capacitor, C_{in}, C_1 and C_2	ECE-T2VP182FA

B. Loss Modeling

The loss modeling for the proposed system shown in Fig. 2 has been carried out by modeling the actual components in PLECS 4.0. The switching components used for the modeling is shown in the Table II,

For the loss modeling of the passive components, the internal resistance of the inductors, L_1, L_2 and L_f are r=100 mΩ and the ESR, R_{HB} for the capacitors $C1$, C_2 and C_{in}

This article has been accepted for publication in a future issue of this journal, but has not been fully edited. Content may change prior to final publication. Citation information: DOI 10.1109/TIE.2017.2784396, IEEE Transactions on Industrial Electronics

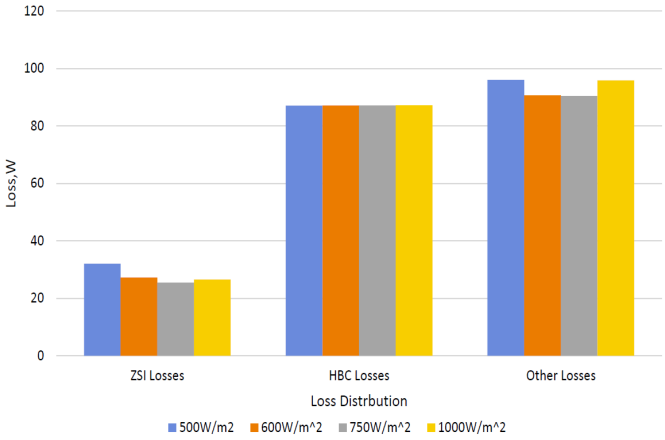

Fig. 9. Loss distribution chart for the MZSI topology for a fixed charging power P_B=3.3 kW at 25 °C, under varying irradiation

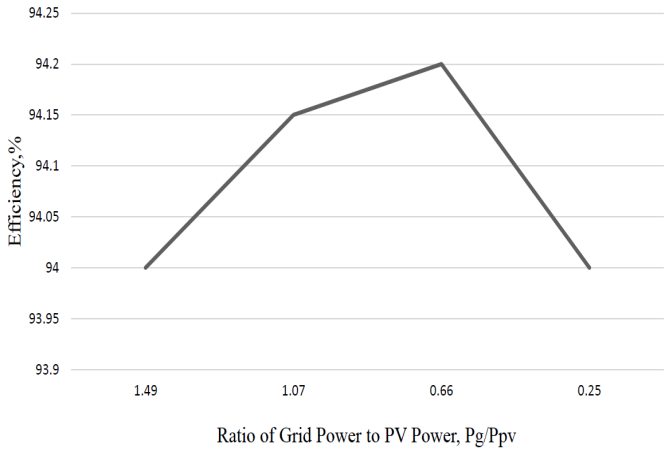

Fig. 10. Efficiency curve for different ratios of AC Grid Power P_g to Photovoltaic Power P_{pv} curve for a fixed charging power P_B=3.3 kW at 25 °C under varying irradiation

are 138 mΩ.

Fig. 9 shows the loss distribution between the ZSI (conduction and switching losses of the MOSFETs and diode D), the HBC (conduction and switching losses of the MOSFETs and secondary diodes) and other losses in due to the inductor, capacitors, leakage losses in the high frequency transformer and battery series resistances in the system for varying irradiations for a constant charging power P_B=3.3 kW.

Fig. 10 shows the efficiency is around 94% from the efficiency curve for various ratios of AC Grid Power,P_g, to Photovoltaic Power, P_{pv} for a fixed charging power, P_B=3.3 kW at 25 °C, for varying irradiation between $500W/m^2$ to $1000W/m^2$. Although the efficiency variations is small, the efficiency is the highest when the sharing between the photovoltaic power P_{pv} and the grid power P_g is equal.

For a constant frequency of operation,the HBC MOSFET losses remain constant for a fixed value V_B and charging power,P_B. Although in reality, this might not be the case. The efficiency of the converter will change with the change in the battery voltage. Fig. 11 shows the distribution of the losses beween the ZSI losses,the HBC MOSFETs and the losses due

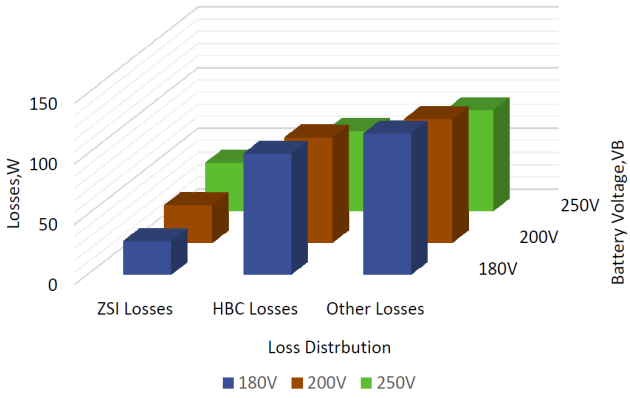

Fig. 11. Loss distribution for various battery voltages,V_B, for a fixed charging power,P_B=3.3 kW, at 45 °C

TABLE III
MODIFIED ZSI BASED CHARGER SYSTEM PROTOTYPE ELECTRICAL SPECIFICATIONS

Parameters	Value
Input Voltage, V_{in}	38 V
Input Current, I_{in}	3.82 A
Inductor Value, L_1 & L_2	500 uH
Peak DC Link Voltage, V_{PN}	63.33 V
Modulation Index, M	0.75
Shoot Through Duty Ratio, D_{0MAX}	0.2
Switching Frequency, F_{SW}	25 kHz
Grid Voltage, V_g	34 V(RMS)
Inverter Output Filter Inductor, L_f	2.5 mH
HBC switching frequency, f_{HBC}	50 kHz

to the inductor,capacitors,leakage losses in the high frequency transformer and battery series resistances in the system for various battery voltages. From Fig.11,at 45 °C, the v_{pv} drops to 258V and it can be observed that with the increase in battery voltage the ZSI losses increase but the HBC losses and the losses in the passive components reduce.

C. Experimental Verification of the MZSI power balance operation

In this paper as proof of concept, a scaled down 175W experimental setup was built using MATLAB/Simulink and dSPACE 1103.The setup has the following specifications shown in table III.

Fig. 12 shows the PWM scheme for the HBC. Each of the split primary operate for half the HBC switching period. Each MOSFET S_{AHB}, S_{BHB}, S_{CHB} and S_{DHB} operates exclusively for one quarter of the entire HBC switching period. Equation (23) can be written in terms of the current sharing between the AC load(grid) and the battery as:

$$i_{PV} = \frac{1 - D_0}{2(1 - 2D_0)} i_b + \frac{M}{\sqrt{2}(1 - 2D_0)} i_g \qquad (21)$$

where M is the modulation index and D_0 is the shoot through duty ratio. For D_0=0.2,

$$i_{PV} = \frac{2}{3} i_b + \frac{\sqrt{3}}{2} i_g \qquad (22)$$

This article has been accepted for publication in a future issue of this journal, but has not been fully edited. Content may change prior to final publication. Citation information: DOI 10.1109/TIE.2017.2784396, IEEE Transactions on Industrial Electronics

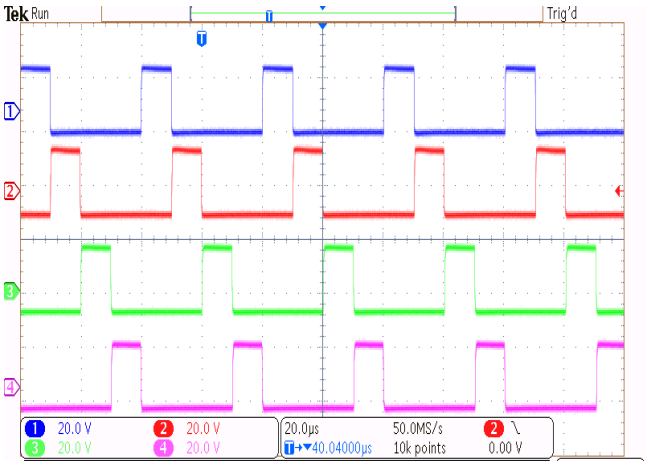

Fig. 12. PWM logic for the isolated HBC

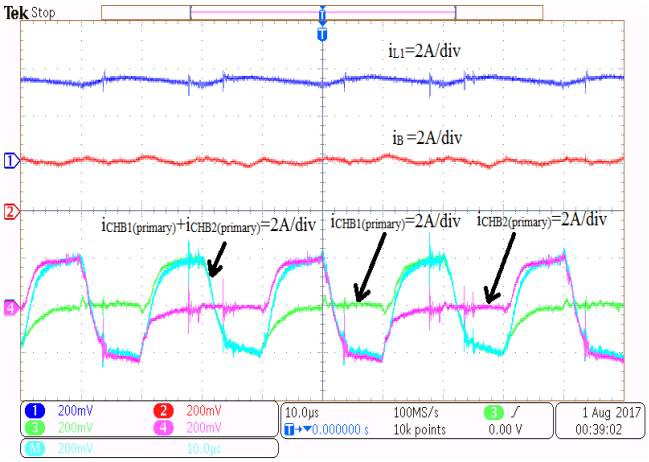

Fig. 13. Experimental setup waveforms for the Inductor current(top), charger output current(middle) and the primary currents of the split charger(bottom)

From equation (22), at D_0=0.2, for an input current i_{PV}=3.82 A and fixed HBC output current i_b=2 A, the ZSI AC output current i_g is calculated to be 2.87 A.

Fig.13 shows the the inductor current i_{L1}, the battery current i_B and the split primary current i_{CHB1} and i_{CHB2} and the total primary current. Each of the primary operate alternately. The total primary current is a high frequency alternating current of f_{HBC}=50 kHz.

From Fig. 13 and Fig. 14, the charger ouput current is maintained at 2 A using a Chroma Programmable AC/DC Electronics Load(Model 6304). The PV input current is maintained at 3.82 A using a Magna-power LXI^{TM} solar emulator. The output grid current is observed to be 2.66 A. Fig. 15 shows the experimental setup for the proof of concept.

The lower values of the output current is a result of the losses in the circuit. The practical PI values for the AC side current control was K_P=0.03 and the battery loop was K_{PB}=.0003 and K_{IB}=.09 and the input PV current loop were K_{Pin}=0.005 and K_{Iin}=2.

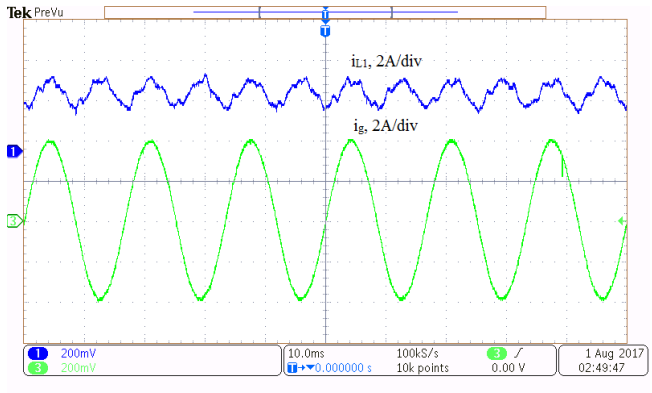

Fig. 14. Experimental waveform input current(blue) and output current(green) between the charger and the AC output of the MZSI

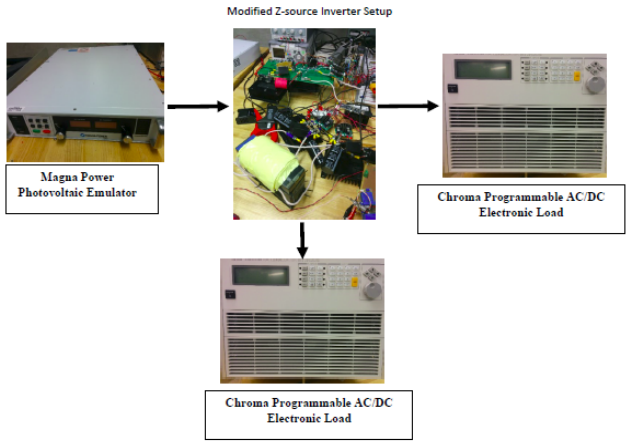

Fig. 15. Experimental setup

TABLE IV
ISOLATED HALF BRIDGE DC-DC SYSTEM ELECTRICAL SPECIFICATIONS

Parameters	Value
Input Voltage, V_C	50.667 V
Output Voltage , V_B	25.335 V
Switching Frequency, $F_{sw(HB}$	50 kHz
Filter inductor, L_B,	330 uH

V. CONCLUSION

A modified ZSI topology has been proposed in this paper is an attractive solution for photovoltaic grid connected charging systems. It consist of a single stage photovoltaic grid (PV-Grid) connection and an integrated charger for PV-Grid connected charging or energy storage. This topology can be applied to centralized configuration for charging in semi-commercial locations such as a parking lot of a shopping mall. For residential applications, this idea can be extended to string inverters with the charger side of the string inverter configurations connected in series or parallel for current sharing. The paper proposes a an energy storage topology using Z source converter through symmetrical operation of its impedance network.

REFERENCES

[1] D. Aggeler, F. Canales, H. Zelaya, D. L. Parra, A. Coccia, N. Butcher, and O. Apeldoorn, "Ultra-fast dc-charge infrastructures for ev-mobility and future smart grids," in *Proc. of IEEE PES Innovative Smart Grid Technologies Conference Europe*, pp. 1–8, Oct. 2010.

[2] G. Carli and S. S. Williamson, "Technical considerations on power conversion for electric and plug-in hybrid electric vehicle battery charging in photovoltaic installations," *IEEE Trans. on Ind. Electron.*, vol. 28, no. 12, pp. 5784–5792, 2013.

[3] J. G. Ingersoll and C. A. Perkins, "The 2.1 kw photovoltaic electric vehicle charging station in the city of santa monica, california," in *Proc. of the Twenty Fifth IEEE Photovoltaic Specialists Conference*, pp. 1509–1512, May. 1996.

[4] S. B. Kjaer, J. K. Pedersen, and F. Blaabjerg, "A review of single-phase grid-connected inverters for photovoltaic modules," *IEEE Trans. on Ind. Appl.*, vol. 41, no. 5, pp. 1292–1306, Sep. 2005.

[5] N. A. Ninad, L. A. C. Lopes, and I. S. Member, "Operation of Single-phase Grid-Connected Inverters with Large DC Bus Voltage Ripple," *Proc. of the IEEE Canada Electrical Power Conference*, 2007.

[6] S. Bai, D. Yu, and S. Lukic, "Optimum design of an ev/phev charging station with dc bus and storage system," in *Proc. of IEEE ECCE*, pp. 1178–1184, Sep. 2010.

[7] F. Z. Peng, "Z-Source Inverter," *in IEEE Trans. on Ind. Appl.*, vol. 39, no. 2, pp. 504–510, 2003.

[8] Y. Huang, M. Shen, F. Z. Peng, and J. Wang, "Z-source inverter for residential photovoltaic systems," *IEEE Trans. on Power Electron.*, vol. 21, no. 6, pp. 1776–1782, Nov. 2006.

[9] S. A. Singh, N. A. Azeez, and S. S. Williamson, "Capacitance reduction in a single phase quasi z-source inverter using a hysteresis current controlled active power filter," in *in Proc. of IEEE 25th Int. Symp.on Ind. Electron.*, pp. 805–810, Jun. 2016.

[10] S. A. Singh, G. Carli, N. A. Azeez, and S. S. Williamson, "A modified z-source converter based single phase pv/grid inter-connected dc charging converter for future transportation electrification," in *Proc. of IEEE ECCE*, pp. 1–6, Sep. 2016.

[11] Y. Li, S. Jiang, J. G. Cintron-Rivera, and F. Z. Peng, "Modeling and control of quasi-z-source inverter for distributed generation applications," *IEEE Trans. on Ind. Electron.*, vol. 60, no. 4, pp. 1532–1541, Apr. 2013.

[12] T. Chandrashekhar and M. Veerachary, "Control of single-phase z-source inverter for a grid connected system," in *Proc. of Int. Conf. on Power Syst.*, pp. 1–6, Dec. 2009.

[13] B. Ge, Y. Liu, H. Abu-Rub, R. S. Balog, F. Z. Peng, S. McConnell, and X. Li, "Current ripple damping control to minimize impedance network for single-phase quasi-z source inverter system," *IEEE Trans. on Ind. Info.*, vol. 12, no. 3, pp. 1043–1054, Jun. 2016.

[14] B. Ge, H. Abu-Rub, F. Z. Peng, Q. Lei, A. T. de Almeida, F. J. T. E. Ferreira, D. Sun, and Y. Liu, "An energy-stored quasi-z-source inverter for application to photovoltaic power system," *IEEE Trans. on Ind. Electron.*, vol. 60, no. 10, pp. 4468–4481, Oct. 2013.

[15] J. Rabkowski, R. Barlik, and M. Nowak, "Pulse width modulation methods for bidirectional/high-performance z-source inverter," in *Proc. of IEEE Power Electron. Spec. Conf.*, pp. 2750–2756, Jun. 2008.

[16] S. Dong, Q. Zhang, and S. Cheng, "Analysis of critical inductance and capacitor voltage ripple for a bidirectional z -source inverter," *IEEE Trans. on Power Electron.*, vol. 30, no. 7, pp. 4009–4015, Jul. 2015.

[17] M. Trabelsi and H. Abu-Rub, "A unique active anti-islanding protection for a quasi-z-source based power conditioning system," in *Proc. of IEEE Appl. Power Electron. Conf.e and Expo.*, pp. 2237–2243, Mar. 2015.

Siddhartha A. Singh (S' 10) is currently pursuing the Ph.D. degree in electrical engineering with the Smart Transportation Electrification and Energy Research Group, Department of Electrical, Computer, and Software Engineering, University of Ontario Institute of Technology, Oshawa, ON, Canada. His current research interests include photovoltaic converters, electric vehicle battery chargers, and power electronics converter development.

Giampaolo Carli is a power electronics specialist presently working in the domain of high-voltage generation for x-ray systems at EMD Technologies in Saint-Eustache, Canada. After receiving a Bachelors degree in Electrical Engineering at McGill University in 1984, he devoted many years to the power electronics industry in various fields ranging from industrial and commercial computer systems, telecom, and LED lighting. In 2009 he obtained a M.S. in electrical engineering from Concordia University in Montreal with specialization in electric vehicle charging technology and infrastructure. Besides his technical pursuits, he also enjoys playing and composing music, as well as the study of physics, metaphysics and philosophy.

Najath A. Azeez (M'99-SM'04-F'09) received the B.Tech degree from the National Institute of Technology, Calicut, India, in 2003, and the M.Tech. and Ph.D. degrees from the Indian Institute of Science, Bangalore, India, in 2008 and 2014, respectively. He is currently working as a Postdoctoral Fellow at the University of Ontario Institute of Technology (UOIT), Oshawa, ON, Canada. His research interests include the areas of power converters and drives.

Sheldon S. Williamson (S'01-M'06-SM'13) is currently a Professor with the Smart Transportation Electrification and Energy Research Group, Department of Electrical, Computer, and Software Engineering, University of Ontario Institute of Technology, Oshawa, ON, Canada. His current research interests include advanced power electronics and motor drives for transportation electrification, electric energy storage systems, and electric propulsion. Dr. Williamson holds the prestigious NSERC Canada Research Chair position in Electric Energy Storage Systems for Transportation Electrification.